Concepts for Experiments at Future Colliders I

PD Dr. Oliver Kortner

15.12.2024

Strip and pixel sensors

Silicon strip sensors

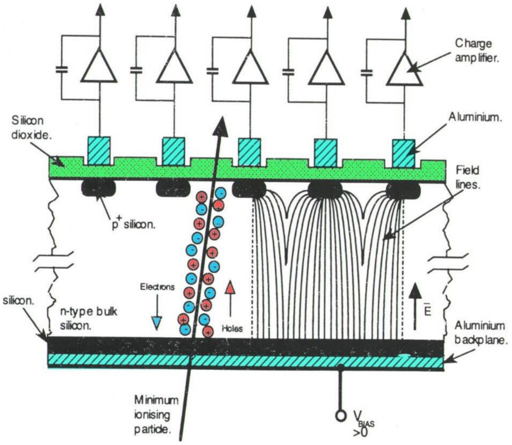

Silicon pixel sensors

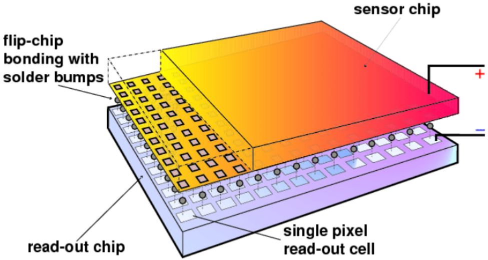

Monolithic sensors

Hybrid sensor

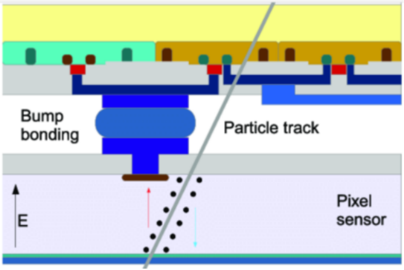

- Sensor and amplifier chip are two separate devices.
- Concept successfully used at the (HL)-LHC: required resolution, speed, granularity, radiation hardness.
- Disadvantage for the FCC-ee where radiation hardness is not an issue: a lot of extra material due to the amplifier chip

Monolithic sensor

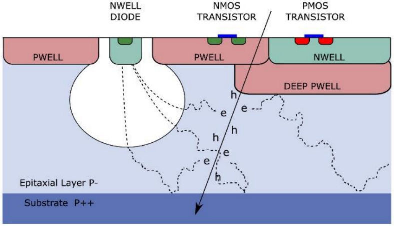

- Sensor and amplifier combined in one device.
- Main advantage: reduction of material.

Recapitulation of the previous lecture

Functions of an inner detector

Tasks

- Measurement of the charge q and the momentum $\vec{p}$ of a charge particle.
- Measurement of the particle's origin/vertex.

Basic structure of an inner detector

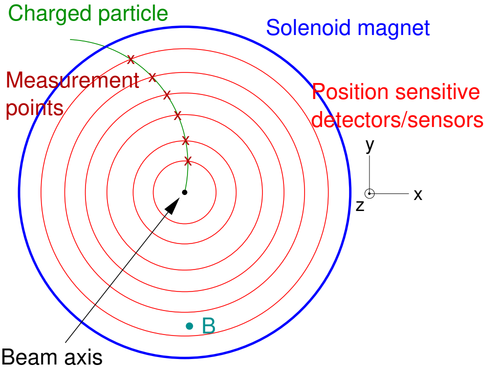

Parameters of the reconstructed track

- Sign of the curvature $\rightarrow$ sgn(q).
- Size of the curvature $\rightarrow p$.
- Direction close to the beam axis $\rightarrow \vec{p}/p$.
- Distance of the track from the beam axis $\rightarrow$ Vertex of the particle.

Recapitulation of the previous lecture

Momentum resolution of an inner detector

- Recapitulation:

$$\frac{\delta\left(\frac{q}{p}\right)}{q/p} = \left.\frac{\delta\left(\frac{q}{p}\right)}{q/p}\right|_{Multiple\ \ scattering} \oplus \left.\frac{\delta\left(\frac{q}{p}\right)}{q/p}\right|_{Spatial\ \ resolution}.$$

  - $\left.\frac{\delta\left(\frac{q}{p}\right)}{q/p}\right|_{Multiple\ \ scattering}$ independent of $\frac{q}{p}$. $\left.\frac{\delta\left(\frac{q}{p}\right)}{q/p}\right|_{Spatial\ \ resolution} \propto \frac{p}{|q|}$.

Momentum resolution of an inner detector

- Recapitulation:

$$\frac{\delta\left(\frac{q}{p}\right)}{q/p} = \frac{\delta\left(\frac{q}{p}\right)}{q/p}\Bigg|_{Multiple\ \ scattering} \oplus \frac{\delta\left(\frac{q}{p}\right)}{q/p}\Bigg|_{Spatial\ \ resolution}.$$

  - $\frac{\delta\left(\frac{q}{p}\right)}{q/p}\Big|_{Multiple\ \ scattering}$ independent of $\frac{q}{p}$. $\frac{\delta\left(\frac{q}{p}\right)}{q/p}\Big|_{Spatial\ \ resolution} \propto \frac{p}{|q|}$.

- Estimation of $\frac{\delta\left(\frac{q}{p}\right)}{q/p}\Big|_{Spatial\ \ resolution}$:

$$\frac{\delta\left(\frac{q}{p}\right)}{q/p}\Bigg|_{Spatial\ \ resolution} \approx \frac{\sigma 2\sqrt{5}}{BL^2\sqrt{n}} \cdot \frac{p}{|q|};$$

σ: Spatial resolution of a single measurement plane.
B: Magnetic field strenght in the inner detector.
L: Radius of the inner detector.
n: Number of (equidistant) measurement planes.

Recapitulation of the previous lecture

Impact parameter

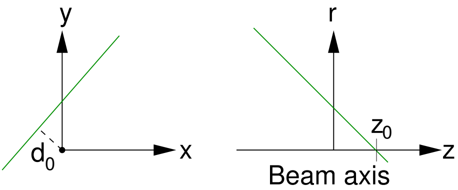

Nomenclature

- d_0: Transverse impact parameter.
- z_0: Longitudinal impact parameter.

Conventions

d_0 and z_0 are expressed either relative to the average collision point or relative to the primary vertex.

Recapitulation of the previous lecture

Impact parameter

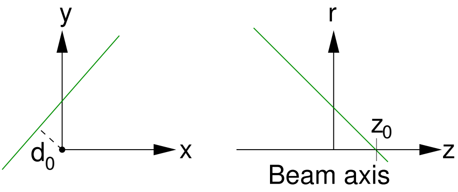

Nomenclature

- d_0: Transverse impact parameter.
- z_0: Longitudinal impact parameter.

Conventions

d_0 and z_0 are expressed either relative to the average collision point or relative to the primary vertex.

Requirements for the innermost detector plane for the d_0- and z_0 measurements

- Simplifying assumptions
  - Consider z_0 measurement.
  - Tracks are straight close to (0,0,0).
  - Two detector planes at r_1 and r_2 with spatial resolutions σ_1 and σ_2.
- z_0 resolution

$$\sigma_{z_0} = \frac{\sqrt{r_2^2\sigma_1^2 + r_1^2\sigma_2^2}}{|r_2 - r_1|} \oplus \sigma_{Multiple\ scattering}.$$

$\Rightarrow$ Thin layers close to the beam axis with high momentum resolution to maximize σ_{z_0}.

Recapitulation of the previous lecture

Basic parameters of the HL-LHC and the FCC

Centre-of-mass energy and luminosity

Collider	$\sqrt{s}$ [TeV]	$\mathcal{L}_{max}$ [cm^{-2}s^{-1}]	$\int \mathcal{L}dt$ [ab^{-1}]
HL-LHC	14	$7,5 \cdot 10^{34}$	3
FCC, phase 1	100	$5 \cdot 10^{34}$	2,5
FCC, phase 2	100	$30 \cdot 10^{34}$	15

Scenarios

- HL-LHC: 2026 bis 2036.
- FCC, phase 1: 10 years of operation.
- FCC, phase 2: 15 years of operation.

Number $N_{pile-up}$ of inelastic pp collisions per bunch crossing

- HL-LHC: 140 (bunch crossings every 25 ns).
- FCC, phase 1:
  - 170 (bunch crossings every 25 ns).
- FCC, phase 2, 2 scenarios:
  - 1020 (bunch crossings every 25 ns).
  - 204 (bunch crossings every 5 ns).

Recapitulation of the previous lecture

Minimum-bias events at the FCC and the HL-LHC

Radiation levels in the detectors depend on the structure of minimimum-bias events (simplified: "inelastice pp collisions without a hard scatter).

Cross section of inelastice pp collisions

- $\approx$80 mb at $\sqrt{s}$=14 TeV.
- $\approx$100 mb at $\sqrt{s}$=100 TeV, hence 25% larger than at the HL-LHC.

Charged particle multiplicity per rapidity unit

- $\approx$5,4 at $\sqrt{s}$=14 TeV.
- $\approx$8 at $\sqrt{s}$=100 TeV, hence 1.5 times larger than at the HL-LHC.

Average partiple momentum

- $\approx$0.6 GeV at $\sqrt{s}$=14 TeV.
- $\approx$0.8 GeV at $\sqrt{s}$=100 TeV, hance 1.3 times larger than at the HL-LHC.

Minimum-bias events at the FCC are very similar to those at the LHC.

$\Rightarrow$ Operation conditions in phase 1 of the FCC very similar to the operation conditions at the HL-LHC.

Radiation levels in the inner detector

Inner detector: Radiation levels in the first pixel detector layer ($r = 3.7$ cm)

	HL-LHC (3 ab^{-1})	FCC, phase 1	FCC, phase II
1 MeV-neq flux [cm^{-2}]	$1.5 \cdot 10^{16}$	$3 \cdot 10^{16}$	$3 \cdot 10^{17}$
Dose [MGy]	4.8	9	90

$\Rightarrow$ Semiconductor detector for the HL-LHC are also suitable for the first phase of the FCC. Development of more radiation hard detector neccessary for the second phase of the FCC.

Recapitulation of the previous lecture

Radiation damage of silicon detectors

The huge fluxes of charged and neutral particles in the inner detector cause damages of the semiconductor detectors.

Two mechanisms

- Damage of the surface and boundary surfaces of semiconductor detectors and of the read-out chips by ionizing radiation.
  As the ionization is a resersible process in a semiconductor, no permant damages of the crystal.
- Scattering off the atoms of the crystal lattice can cause atom displacements and other damages of the crystal lattice.

Convention

The damage of the substrate by scattering off the atoms is expressed as the damage of neutrons with 1 MeV energy.

Damages of the substrate

- Lattice atoms can be displaced by collisions with the radiation background leading to empty places and atoms on inter-lattice points as primary point defects.

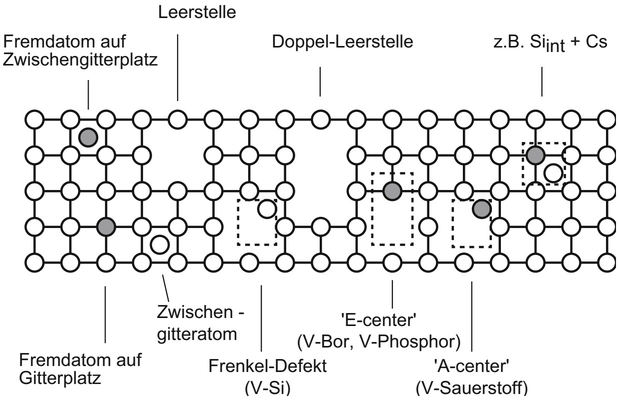

- Most of the primary defects are instable and disappear by recombination.
- Due to their mobility primary point defects can build stable defect complexes with impurity atoms.

Consequences of substrate damages

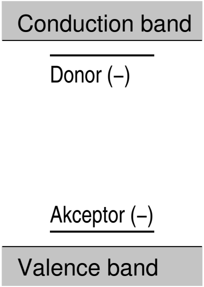

Creation of acceptor and donor centres

- Charged defects which act as acceptor or Donor centres.

⇒ Modification of the effective doping concentration.

⇒ Modification of the depletion region and the depletion voltage. Type inversion is possible.

Type inversion by acceptor and donor centres

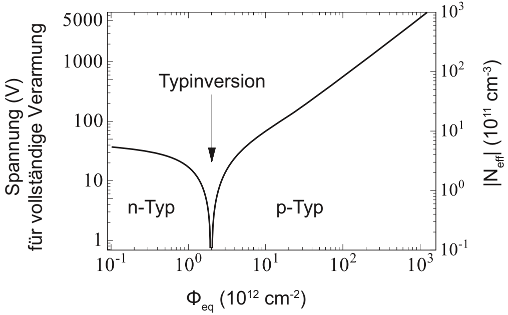

Type inversion already after few years of operation at the LHC.

⇒ The value of the depletion voltage changes with time. After a long operation of the detectors, only partial depletion possible leading to loss of signal.

Recapitulation of the previous lecture

Consequences of substrate damages

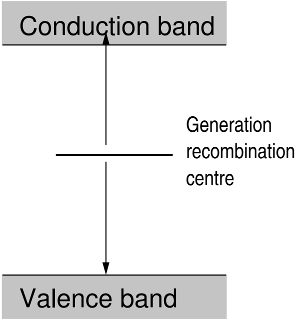

Creation of generation recombination centres

- Impurity levels in the middle of the band gap act as generation and recombination centres.
- generation centres increase the leakage current.

⇒ Increased detector noise and detector temperature.

- Danger of destroying the detector by a chain reaction of a leakage current induced temperature increase and a temperature induced increase of the leakage current.

Consequences of substrate damages

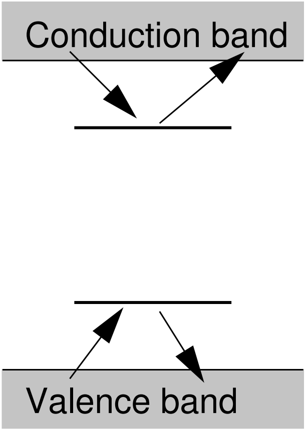

Creation of trapping centres

- Trapping of electrons and hole in impurity levels.

⇒ Reduced life time and mean free path of the charge carriers.

⇒ Signal loss if the trapping takes longer than the creation of the signal.

Measures to increase the radiation hardness

Cooling of the sensors

- Damages of the substrate are temperature dependent.

⇒ Damages can be cured by heating up the crystal. But too long heating can convert harmless impurities to harmful impurities.

⇒ Second process can be suppressed by operating the sensors at low temperatures $\sim$-10^{o}C.

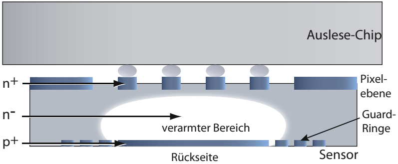

(a) n^--Substratdotierung vor der Bestrahlung.

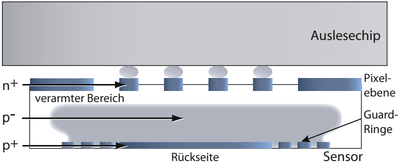

(b) p^--Subatratdotierung nach der Bestrahlung.

n^+-on-n- or n^+-on-p sensors

- After type inversion complete depletion no longer possible.

⇒ n^+-on-n or n^+-on-p sensoren to have the n^+p layer on the side of the read-out electrode.

Measures to increase the radiation hardness

Enrichment of the silicon substrate with oxygen

- Suppression or prevention of type inversion by enrichment of the silicon substrate with oxygen.

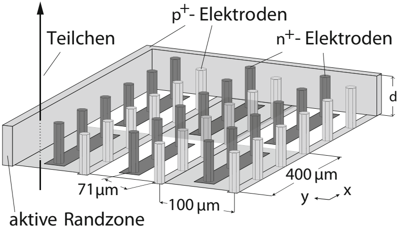

Thin sensors or 3-D pixel sensors

- Goal: Reduction of drift paths and acceleration of the charge collection to oppose trapping effects.
- Two possibilities: Thin planar sensors or 3D pixel sensors with column electrodes.

Signal formation in a semiconductor detector

- The charge measured at the electrodes of a semiconductor detector, denoted as Q, is the induced charge generated by the movement of liberated charge carriers (q).
- The calculation of the induced charge involves the use of the Shockley-Ramo theorem, which we will not derive today.
- Today, we present a simplified derivation:
  - Work done by the electric field on q: $qE(x)dx$.
  - Change in the electric field energy in a capacitor: $\frac{Q}{C}dQ = UdQ$.
  - Due to conservation of energy, $qE(x)dx = UdQ$.
  - In a plate capacitor with plate spacing D, $E = \frac{U}{D}$, leading to the equation

$$dQ = \frac{q}{D}dx$$

    for the infinitesimal induced charge dQ.

Temporal evolution of the induced charge

- Average velocity of electrons and holes:

$$v_{e/h} = q_{e/h} E \tau_{e/h},$$

  where τ is the mean time between two collisions of charge carriers in the lattice.

- Electric field in a pn junction from a p-substrate with an n$^+$-doped side:

$$E = -\frac{eN_A}{\epsilon} x.$$

⇒

$$v_{e/h} = \frac{dx_{e/h}}{dt} = \pm \frac{e^2 N_A}{\epsilon} x_{e/h} = C_{e/h} x_{e/h},$$

hence

$$x_{e/h}(t) = x_0 e^{C_{e/h} t}.$$

Temporal Evolution of the Induced Charge

- $Q_{e/h}(t) = \int_0^t \frac{q_{e/h}}{D} v(t')dt' = \frac{q_{e/h}}{D} x_0 (e^{C_{e/h}t} - 1).$

Leo 1994

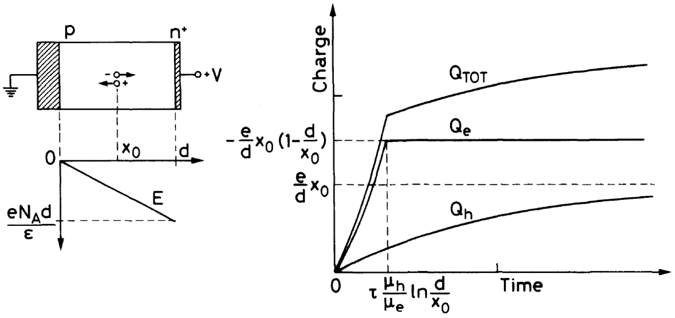

Fig. 10.10. Signal pulse shape due to a single electron-hole pair in an np junction

- $C_e > 0,\ q_e < 0.$
- $C_h < 0,\ q_h > 0.$

Structure of a hadron collider experiment

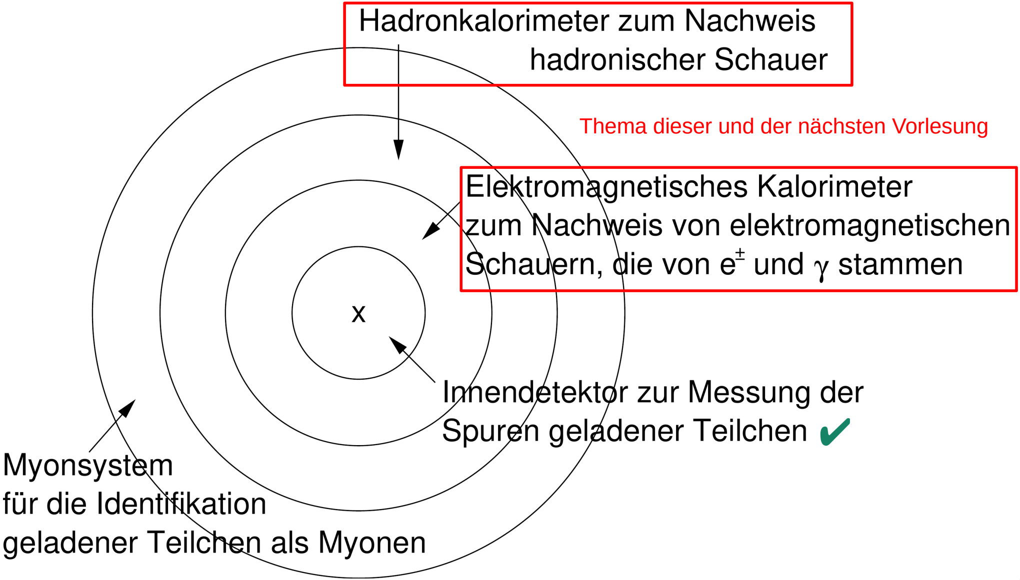

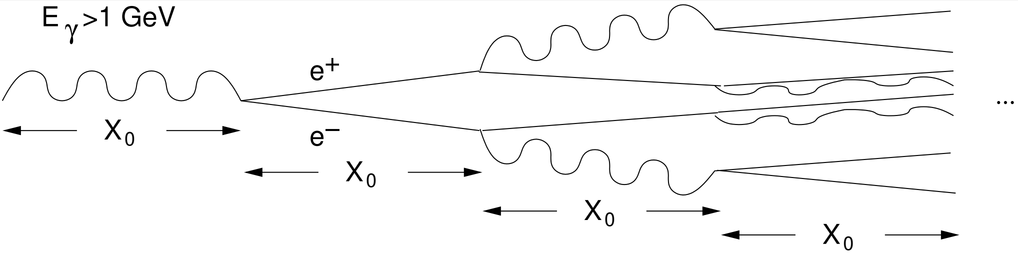

- After a distance $n \cdot X_0$: 2^n particles with energy $E_n \approx \frac{E_\gamma}{2^n}$.
- End of the cascade (shower), if $E_n = E_k$: $n = \frac{\ln \frac{E_\gamma}{E_k}}{\ln 2}$.
- Shower length: $n \cdot X_0 = X_0 \cdot \frac{\ln \frac{E_\gamma}{E_k}}{\ln 2}$.

Example

- $E_\gamma = 100$ GeV.
- Material: iron, d.h. $X_0 \approx 2$ cm, $E_k \approx 20$ MeV.

$\Rightarrow$ $n = 12$, d.h. ~ 4000 particles.
Shower length: $L_{longitudinal} \approx 24$ cm.

The full treatment with massive electrons and positrons leads to the following result.

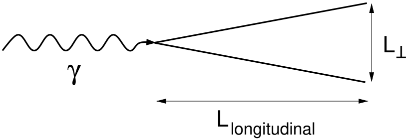

$$L_\perp \approx 4R_M = 4X_0 \frac{21,2 \text{ MeV}}{E_k}$$

R_M: Molière radius

- The transvers size of the shower $L_\perp$ is independent of $E_{\gamma/e^\pm}$.
- $L_{T,Fe} = 4 \cdot 1,8$ cm $\cdot \frac{21{,}2\text{MeV}}{30{,}2\text{MeV}} \approx 5$ cm.
- Characteristic for electromagnetic showers: small transverse size which is independent of $E_{\gamma,e^\pm}$.
- The number of generated particles is a measure for $E_{\gamma,e^\pm}$ and proportional to $E_{\gamma,e^\pm}$.

Hadron showers

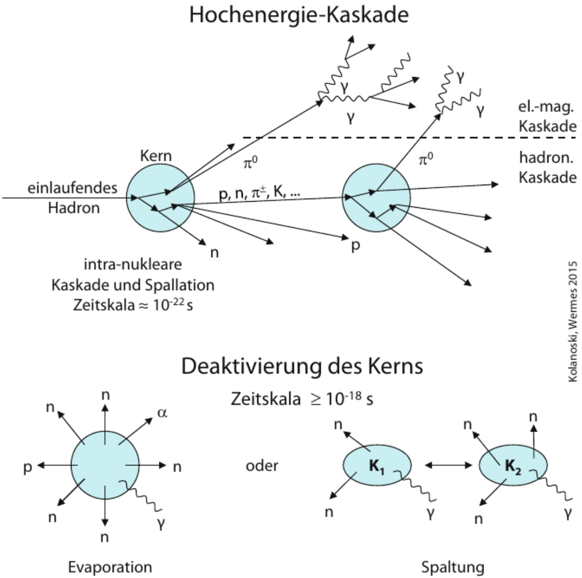

Similar behaviour like electromagnetic showers:

- Shower length proportional to $\lambda_A \approx 35 \text{ g cm}^{-2} \frac{A^{1/3}}{\rho} \gg X_0$.
- Transverse size independent of the energy of the primary hadron: λ_A.
- But much stronger variations of the shower size than in case of electromagnetic showers.

Shower components and shower fluctuations

Contributions to the energy E_{dep} deposited in a block of material

$$E_{dep} = \underbrace{(f_{em} + \underbrace{f_{ion} + f_n + f_\gamma + f_B}_{=: f_h})}_{=1 \text{ per definitionem}} E_{dep}$$

- f_{em}. Fraction of the energy deposited by photons from π^0 decays. As neutral pions are created again and again, f_{em} increases with the particle multiplicity in the cascade, hence with the energy of the incoming hadron.
- f_{ion}. Fraction of the energy deposited by a charged shower particle by ionization.
- f_n. Fraction of the energy deposited by neutrons via elastic scattering or nuclear reactions.
- f_γ. Fraction of the energy deposited by photons which are created in nuclear reactions. $E_\gamma \sim$ keV...MeV $\Rightarrow$ energy transfer by Compton scattering or photoelectric effect. This contribution can occur with a large delay $\gtrsim \mu$s.
- f_B. The binding energy which is required to break up a nucleus is not measured and does not contribute to the calorimeter signal. One has a similar situation with neutrinos which are usually take into account in f_B.

Shower components and shower fluctuations

Contribution of the energy E_{dep} deposited to a block of matter

$$E_{dep} = \underbrace{(f_{em} + \underbrace{f_{ion} + f_n + f_\gamma + f_B}_{=:f_h})}_{=1 \text{ per definitionem}} E_{dep}$$

- f_{em} varies strongly in a hadronic shower between 0 and 1 if no or only neutral pions are generated in the first interactions.
- The composition of the hadron component is independent of the type and energy of the incoming hadron.

Passage of muons through matter

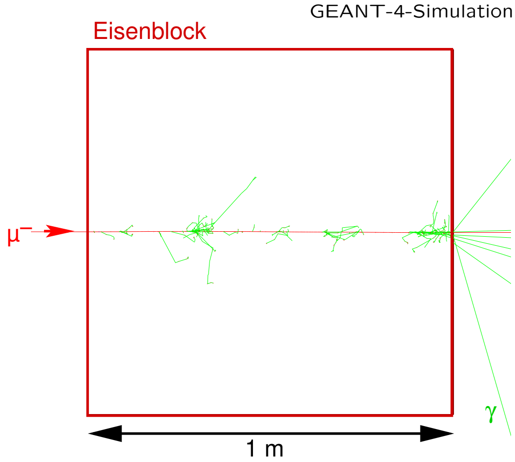

- Muon energy: 10 GeV.
- Muons: only electroweak interaction.
- Muons are heavy particles.

⇒ Small energy loss by excitation and ionization of iron atoms.

⇒ Muon passes the entry iron block.

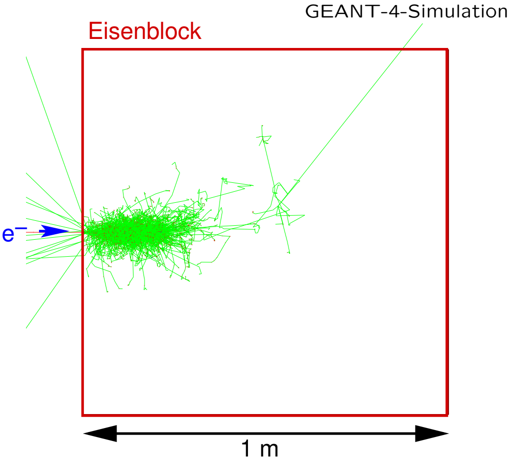

- Electron energy: 10 GeV.
- Electrons: only electroweak interaction.

⇒ Large energy loss mainly by bremsstrahlung.

⇒ Evolution of an electron photon shower.

⇒ The electrons is stopped in the iron block.

Passage of pions through matter

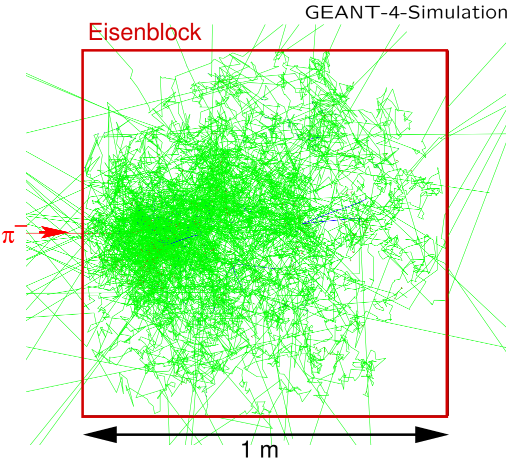

- Pion energy: 10 GeV.
- Charged pions: electroweak and strong interaction.
- Charged pions are heavy charged particles.

⇒ Small energy loss by excitation and ionization of iron atoms.

⇒ But development of a hadron shower.

⇒ As the strong interaction is short range, the shower almost completly fill the iron block.

⇒ The block is just thick enough to stop the pion.

Calorimeter types

Nomenclature

Passive medium: Material in which the shower develops.

Aktive medium: Material in which the electronically detectable signals of the shower particles are created.

Two types of calorimeters

- Homogeneous calorimeters, in which the active material also serves as passive material.
- Inhomogeneous calorimeters or sampling calorimeters with alternating layers of active and passive materials.

Hadron calorimeters are always sampling calorimeters in order to limit their size. There are homogeneous and inhomgeneous electromagnetic calorimeters.

Longitudinal segmentation of a calorimeter

- Electromagnetic calorimeters are segmented longitudinally in order to be able to measure the longitudinal shower shape. This allows for the discrimination of showers initiated by electrons from showers initiated by pions which are longer than electron showers.
- In hadron calorimeters, the longitudinal segementation is important for the discrimination of the different shower components.

Tailcatcher, Presampler, lateral structure

Tailcatcher

This is a longitudinal extension of a calorimeter for the rough measuremetner of the shower tails to minimize detection losses.

Presampler

This is used in front of an electromagnetic calorimeter to identify if a shower initiated by a photon started before the calorimeter.

Lateral structure

The lateral segmentation has to be chosen small enough to separate neighbouring shower. So the segmentation is given by the Moliére radius for electromagnetic calorimeters and by the nuclear interaction length for hadron calorimeters.

Energy resolution and linearity

Energy resolution

- The energy measurement in a calorimeter consist of the detection of the shower particles. The measured energy is proportional to the number of detected shower particles N leading to $\frac{\delta E}{E} = \frac{\delta N}{N} = \frac{1}{\sqrt{N}}$.
- In a real calorimeter contributions to the energy resolution from detector noise and mechanical and electronic non-uniformities must be taken into account:

$$\frac{\delta E}{E} = \frac{a}{\sqrt{E}} \oplus \underbrace{\frac{b}{E}}_{El.\ noise} \oplus \overbrace{c}^{Non-uniformities}$$

Linearity

Not only $\frac{\delta E}{E}$ is important, but also that the measureed signal depends linearly on E.